Histol Histopathol (2023) 38: 1017-1028

Histology and Histopathology
From Cell Biology to Tissue Engineering

ORIGINAL ARTICLE Open Access

Hsa_circ_0026344 suppresses gastric cancer progression via modulating the miR-1290/FBP2 axis

GaoChun Xiao[1], TingTing Zhang[2], BinBin Tan[1] and Hu Hao[3]

[1]Department of General Surgery, [2]Department of Clinical Oncology and [3]Department of Gastroenterology, Taihe Hospital, Hubei University of Medicine, Shiyan, Hubei, PR China

Summary. Background. Circular RNAs (circRNAs) are a novel type of noncoding RNAs and play important roles in tumorigenesis, including gastric cancer (GC). However, the functions of most circRNAs remain poorly understood. In our study, we mainly learn the influence of hsa_circ_0026344 (circ_0026344) in GC progression.

Methods. Circ_0026344, miR-1290 and Fructose-1,6-bisphosphatase 2 (FBP2) expression was determined by quantitative real-time polymerase chain reaction (qRT-PCR). GC cell proliferation, migration, and invasion were detected by colony formation, 5-ethynyl-2'-deoxyuridine (EdU), and transwell assays, respectively. The interaction between circ_0026344 and miR-1290 complex was evaluated by RNA pull-down assay. The interaction of miR-1290 with circ_0026344 or FBP2 was detected using dual-luciferase reporter assay. A xenograft model was established to determine the effect of circ_0026344 on GC tumor growth *in vivo*.

Results. Circ_0026344 expression was dramatically decreased in GC cells and tissues. Circ_0026344 overexpression inhibited GC cell proliferation, migration and invasion. MiR-1290 was predicted as a target of circ_0026344 and miR-1290 overexpression attenuated the anti-tumor effect of circ_0026344 on GC cells. Furthermore, we predicted FBP2 as the target of miR-1290. FBP2 knockdown reversed the effects of circ_0026344 knockdown on GC cell malignant behaviors. Functional analysis showed that circ_0026344 upregulated FBP2 expression via miR-1290. Additionally, in vivo studies demonstrated that circ_0026344 suppressed GC tumor progression.

Conclusion. In conclusion, circ_0026344 inhibited GC cell proliferation via the miR-1290/FBP2 axis, which might provide a new therapeutic target for GC patients.

Corresponding Author: Hu Hao, MM. Department of Gastroenterology, Taihe Hospital, Hubei University of Medicine, No. 32, Renmin South Road, Shiyan City, Hubei Province, PR China. e-mail: huhaoth@163.com

www.hh.um.es. DOI: 10.14670/HH-18-564

Key words: Gastric cancer, circ_0026344, miR-1290, FBP2

Introduction

Gastric cancer (GC) is one of the most familiar cancers in the gastrointestinal tract (Bray et al., 2018). GC can occur due to a number of factors, such as smoking (Vainio et al., 1994), continued high salt food intake (Ge et al., 2012) and genetic mutations (Funakoshi et al., 2019). In recent years, with the development of new treatment strategies for GC, its morbidity and mortality have declined steadily (Zhang et al., 2017). However, the age-standardized 5-year survival rate remains in the 20-40% range (Allemani et al., 2018). Therefore, it is necessary to study the molecular mechanism of GC progression and to exploit more effective therapies.

CircRNAs, newly discovered members of the non-coding RNA family, are characterized by covalently closed continuous rings and RNase R resistance (Qu et al., 2015, 2017). CircRNAs are highly stable and exist in all kinds of cell types. More and more RNA-sequencing analyses have confirmed that circRNAs are highly expressed in tumor tissues, including GC tissues (Ouyang et al., 2019). For example, circ_SETD2 repressed breast cancer progression by regulating the miR-155-5p/SCUBE2 axis (Shen et al., 2020). Circ-SMARCA5 suppressed colorectal cancer development via blocking miR-39-3p and enhancing ARID4B (Miao et al., 2020). In GC, hsa_circ_001988 was found to attenuate GC progression both in vitro and in vivo via sponging miR-197-3p (Sun et al., 2021). This evidence points to the important role of circRNAs in cancer. However, a mass of circRNAs still exist in GC and their roles have not been fully studied.

As negative regulators of downstream target genes, miRNAs are subsets of small non-coding RNAs (ncRNAs) (Hu et al., 2019). Previous studies have found that miR-760 (Ge et al., 2019), miR-122-5p (Meng et al., 2020), and miR-4766-5p (Wei et al., 2019) were

downregulated in GC and served an inhibitory role in the development of GC, while miR-616-3p (Gong et al., 2018) and miR-4513 (Ding et al., 2019a) promoted GC cell growth, invasion, and epithelial-mesenchymal transition (EMT).

Fructose-1,6-bisphosphatase 2 (FBP2) encodes a gluconeogenesis regulatory enzyme and has been reported to repress the progression of cervical cancer (Wang et al., 2022), sarcomas (Huangyang et al., 2020) as well as GC (Li et al., 2013). However, the underlying mechanisms of FBP2 in GC progression are barely clear. For this study, the latent complementary sequences between miR-1290 and hsa_circ_0026344 (circ_0026344) or FBP2 was predicted by starBase v2.0 (https://starbase.sysu.edu.cn/starbase2/index.php).

Accordingly, the aim of this study was to investigate whether circ_0026344 mediates GC progression by the miR-1290/FBP2 axis. Our results showed the downregulation of circ_0026344 in GC samples and cell lines. Furthermore, the upregulation of circ_0026344 inhibited GC cell proliferation, migration and invasion, which was achieved via sequestering miR-1290 and upregulating FBP2. This study provides a new potential target for GC treatment.

Materials and methods

Tissue collection

The Ethics Committee of Taihe Hospital, Hubei University of Medicine approved this experiment. In this study, GC tissues (n=43) and normal tissues (n=43) were gathered from GC patients who voluntarily signed informed consent forms in Taihe Hospital, Hubei University of Medicine. These samples were collected and stored at -80°C.

Cell culture

GC cells (AGS and HGC-27) and human gastric epithelial cells (GES-1) were acquired from the Type Culture Collection of the Chinese Academy of Sciences (Shanghai, China). RPMI-1640 (Invitrogen, Carlsbad, CA, USA) served as the base culture medium for all cells. To make the growth medium, 1% penicillin/streptomycin (Invitrogen) and 10% FBS (Invitrogen) were added to the base culture medium. These cells were grown in a humid incubator with 5% CO_2 at 37°C.

Quantitative real-time polymerase chain reaction (qRT-PCR)

Total RNA was extracted using the TRIzol reagent (Beyotime, Shanghai, China). PrimeScript Reverse Transcriptase Kit (Invitrogen) was used to prepare cDNA. QRT-PCR was performed using PCR System with SYBR Green (Takara, Dalian China). In this, relative expression was analyzed by $2^{-\Delta\Delta Ct}$ method with glyceraldehyde 3-phosphate dehydrogenase (GAPDH) or U6 as internal reference. Primer sequences used for qRT-PCR are shown in Table 1.

Cell transfection

Circ_0026344 and matched negative control (Vector), mimics of miR-1290 (miR-1290) and matched control (miR-NC), small interfering RNA (si-RNA) specifically targeting FBP2 (si-FBP2) and si-RNA negative control (si-NC) were constructed or synthesized by GenePharma (Shanghai, China) and Ribobio (Guangzhou, China).

Colony formation assay

Transfected AGS and HGC-27 cells were incubated for 14 days after seeding into 6-well plates (500 cells per well). When the cell colonies were visible, the plates were washed twice with phosphate buffered saline (PBS, Sangon, Shanghai, China). The washed cell colonies were then fixed in 95% ethanol and stained with 0.1% crystal violet (Sangon). Colony number was counted immediately after taking photographs.

5-ethynyl-20-deoxyuridine (EdU) assay

The proliferation capacity was measured via EdU Cell Proliferation Kit (Beyotime) and cell nuclei were labeled with Diamidine phenylindole (DAPI, Beyotime). GC cells with synchronous staining of EdU and DAPI were counted as the EdU-positive cells. The pictures of cells were taken by fluorescence microscope (Olympus, Tokyo, Japan).

Transwell assay

The transwell inserts (Corning, Corning, NY, USA) coated with or without Matrigel (Corning) were used to determine cell invasion and migration, respectively. A total of 8×10^4 GC cells were collected and resuspended in serum free RPMI-1640. Cell suspension was added to the upper chambers. The lower compartments were filled

Table 1. Primer sequences used for qPCR analysis.

Name	Primers for qPCR (5'-3')	
hsa_circ_0026344	Forward	CGTACCTGGAGACGCTGTTT
	Reverse	CAGAGGGGTTTGGGTACCAG
FBP2	Forward	CCCACATGCCCTCTTCTGTT
	Reverse	CCATAGAATCGCCTGTGGCT
miR-1290	Forward	TGGATTTTTGGATCAGGGA
	Reverse	CTCAACTGGTGTCGTGGA
GAPDH	Forward	AAGGCTGTGGGCAAGGTCATC
	Reverse	GCGTCAAAGGTGGAGGAGTGG
U6	Forward	CTCGCTTCGGCAGCACATA
	Reverse	CGAATTTGCGTGTCATCCT

with RPMI-1640 containing 10% FBS. After 24h, cells remaining on the upper side of the polycarbonate membrane were removed using a cotton swab, and the numbers of invaded and migrated cells were counted to assess cell invasion and migration abilities. Five random fields were chosen for each group.

Western blot assay

Total protein extracted with RIPA reagent (Beyotime) was quantified by a BCA kit (Beyotime). After separating by 10% SDS-PAGE, proteins were transferred on PVDF membranes (Millipore, Billerica, MA, USA) and blocked by 5% non-fat milk, followed by incubation with the primary antibodies and HRP-conjugated secondary antibody (ab6721, Abcam, Cambridge, MA, USA). The protein signaling was imaged by using an enhanced chemiluminescence (ECL) detection kit (Beyotime). The primary antibodies against Proliferating Cell Nuclear Antigen (PCNA, ab18197), Cyclin E (ab133266), matrix metalloprotein 2 (MMP2, ab97779), MMP9 (ab38898), FBP2 (ab236660) and β-actin (ab8226) were purchased from Abcam.

Dual-luciferase reporter assay

The fragments of circ_0026344 and FBP2 3'UTR consisting of the wild-type (WT) or mutant (MUT) binding sites of miR-1290 were cloned into psiCHECK-2 (Promega, Madison, WI, USA) to generate circ_0026344-WT, circ_0026344-MUT, FBP2 3'UTR-WT and FBP2 3'UTR-MUT. Then the generated vectors were co-transfected into AGS and HGC-27 cells with miR-1290 mimics (miR-1290) or miR-NC, respectively. The fluorescence activity of each group was measured by the Dual-Lucy Assay Kit (Solarbio, Beijing, China) after 48h-transfection.

RNA pull-down

Briefly, miR-1290 mimic-biotin (Bio-miR-1290) and its negative control (Bio-miR-NC) were respectively transfected into GC cells for 48h, and the cell lysis was incubated with streptavidin-coated magnetic beads (Promega) for 4h. The pull-down contexts were washed with lysis buffer and the RNAs were recovered in TRizol (Invitrogen) for qPCR-PCR.

Xenograft assay

AGS (1×10^6) cells transfected with circ_0026344 or Vector were injected subcutaneously into nude mice. The tumor volume was determined every week. After 5 weeks, the mice were euthanized to determine the tumor weight. The expression of circ_0026344, miR-1290 and FBP2 was determined. All animal experiments are supported and approved by the Taihe Hospital, Hubei University of Medicine Animal Ethics Committee.

Immunohistochemistry (IHC) staining assay

The xenograft tumor tissues were prepared into paraffin sections, and the expression of Ki67 was determined by IHC assay according to the instructions of SP Kit (Solarbio).

Statistical analysis

GraphPad Prism 8.0 (GraphPad, La Jolla, CA, USA) was used for data processing. Student's t-test was utilized to analyze differences between 2 groups, and analysis of variance (ANOVA) was utilized to analyze differences of multiple groups. Pearson's correlation analysis was used for linear correlation analysis. The data were finally expressed as the mean ± standard deviation. $P<0.05$ was considered significant.

Results

Circ_0026344 level was decreased in GC tissues and cells

We first measured the abnormally expressed circ_0026344 in GC tissues and cells. According to the circbase (http://www.circbase.org/cgi-bin/simplesearch.cgi), circ_0026344 has a spliced length of 2603 bp, which is located at chr12:52314542-52317145 (Fig. 1A). Next, we collected 43 paired GC tissues and adjacent normal tissues, and detected circ_0026344 expression. As shown in Figure 1B,C, a lower level of circ_0026344 was exhibited in GC tissues than that in normal group. Furthermore, circ_0026344 level was also detected in GC cell lines. Results showed that circ_0026344 level was evidently downregulated in AGS and HGC-27 cells compared with GSE-1 cells (Fig. 1D). These results indicated that circ_0026344 might play a vital role in GC development.

Elevated circ_0026344 expression repressed GC cell proliferation

In view of the reduced expression of circ_0026344 in GC tissues and cells, we further explored the role of circ_0026344 in GC progression via a gain-of-function experiment. QRT-PCR exhibited that circ_0026344 expression was enhanced in AGS and HGC-27 cells transfected with circ_0026344 overexpression vector compared to the control group (Fig. 2A,B). Furthermore, two-dimensional colony formation assays showed that overexpression of circ_0026344 inhibited the colony formation in both AGS and HGC-27 cells (Fig. 2C,D). Consistently, the EdU assay manifested that the proliferation of AGS and HGC-27 cells was significantly inhibited by circ_0026344 elevation (Fig. 2E,F). All results indicated that circ_0026344 was able to curb GC cell proliferation.

Upregulated circ_0026344 lowered the migration and invasion of GC cells

The transwell assay presented that circ_0026344 overexpression inhibited the migration and invasion capacities of AGS and HGC-27 cells (Fig. 3A-D). The data showed that the overexpression of circ_0026344 led to a marked decrease in PCNA, Cyclin E, MMP2 and MMP9 levels in AGS and HGC-27 cells when compared to control group (Fig. 3E,F). Together, these findings revealed that circ_0026344 overexpression suppressed malignant behavior in GC cells.

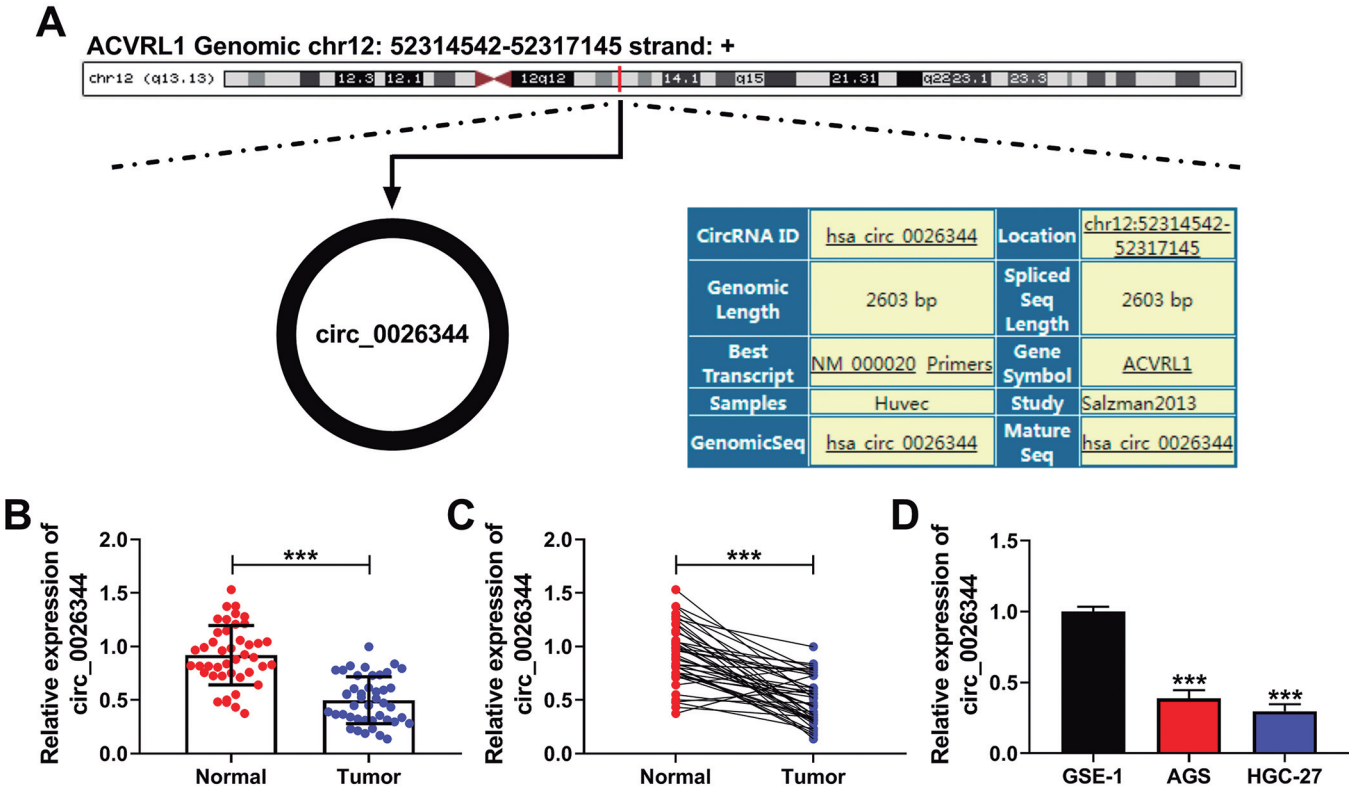

Fig. 1. Circ_0026344 was downregulated in GC tissues and cells. **A.** The location of circ_0026344. **B, C.** The expression of circ_0026344 in tumor tissues and normal tissues was determined using qRT-PCR. **D.** Circ_0026344 expression in GES-1, AGS and HGC-27 cells was measured by qRT-PCR. ***P<0.001.

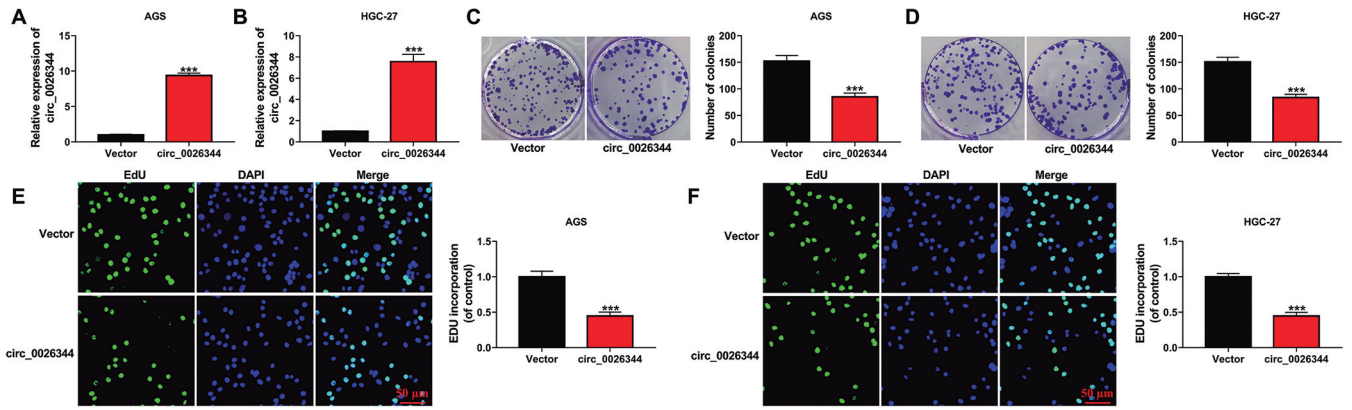

Fig. 2. Circ_0026344 overexpression inhibited GC cell proliferation *in vitro*. **A, B.** QRT-PCR was performed to analyze the expression of circ_0026344 in AGS and HGC-27 cells transfected with circ_0026344 or Vector. **C, D.** Cell colony ability was assessed using colony formation assay. **E, F.** The influence of circ_0026344 on cell proliferation of AGS and HGC-27 cells was evaluated by EdU assay. ***P<0.001.

MiR-1290 was a direct target of circ_0026344

To reveal the underlying molecular mechanism of circ_0026344 in GC, we investigated the interaction between circ_0026344 and miR-1290 in GC cells. QRT-PCR analysis revealed that miR-1290 was accumulated in GC tumor tissues as well as in GC cells (AGS and HGC-27) compared with that in adjacent tissues and GSE-1 cells (Fig. 4A-C). The binding sites of circ_0026344 and miR-1290 were predicted using starBase v2.0 (Fig. 4D). Dual-luciferase reporter assay showed that circ_0026344-WT and miR-1290 cotransfection led to a remarkable suppression in luciferase activity in AGS and HGC-27 cells compared to circ_0026344-WT and miR-NC co-transfected cells, whereas no change was observed in circ_0026344-MUT and miR-1290 cotransfection of GC cells (Fig. 4E,F). Additionally, RNA pull-down assays revealed that the enrichment level of circ_0026344 was remarkably elevated by Bio-miR-1290 in both cell lines (Fig. 4G). Furthermore, we analyzed the correlations between the expression of circ_0026344 and miR-1290 expression in GC tissues. As demonstrated, there was a negative correlation between them (Fig. 4H). Collectively, circ_0026344 interacted with miR-1290 in GC cells.

MiR-1290 upregulation attenuated the circ_0026344 overexpression-induced anti-proliferative effects on GC cells

To explore whether the effect of circ_0026344 was dependent on sponging miR-1290, we first synthesized miR-1290 mimics. As shown in Fig. 5A,B, transfection of miR-1290 mimics efficiently upregulated the expression of miR-1290. To further indicate the role of miR-1290 mimics on circ_0026344-induced anti-tumor effects in GC cells, circ_0026344 and miR-1290 mimics were co-transfected into either AGS or HGC-27 cells for *in vitro* functional studies. Colony formation and EdU assays exhibited that miR-1290 mimics were able to attenuate circ_0026344 overexpression-induced inhibition on cell proliferation (Fig. 5C-F). Collectively, circ_0026344 interacted with miR-1290 to mediate GC cell proliferation.

MiR-1290 overexpression lowered circ_0026344 overexpression-mediated effects on GC cell migration and invasion

Cell migration and cell invasion assays demonstrated that miR-1290 mimics also partially

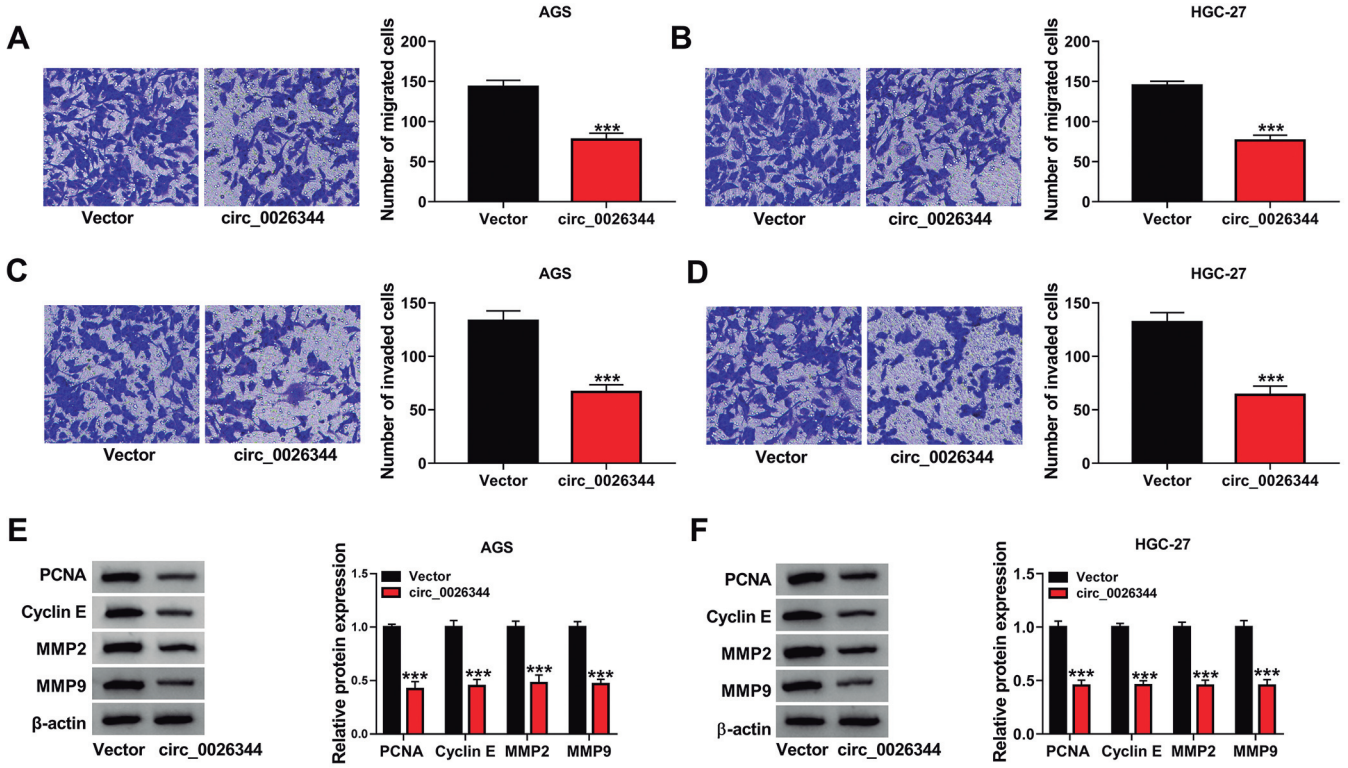

Fig. 3. Upregulation of circ_0026344 inhibited GC cell migration and invasion *in vitro*. **A-D.** Effects of circ_0026344 elevation on cell migration and invasion in AGS and HGC-27 cells were determined by transwell assay. **E, F.** Impacts of circ_0026344 upregulation on the expression of PCNA, Cyclin E, MMP2 and MMP9 proteins of AGS and HGC-27 cells were evaluated by western blot analysis. ***P<0.001.

reversed circ_0026344 overexpression-decreased cell migration and invasion capacities (Fig. 6A-D). The data of western blot assay exhibited that circ_0026344 markedly reduced the levels of PCNA, Cyclin E, MMP2 and MMP9 in AGS and HGC-27 cells, whereas miR-1290 partly reversed the reduction (Fig. 6E,F). All these results suggested that circ_0026344 played a crucial role in GC via sponging miR-1290.

Circ_0026344 regulated FBP2 expression via sponging miR 1290

To investigate whether circ_0026344 inhibited GC cell function by regulating the downstream target genes of miR-1290. The mRNA and protein levels of FBP2 in GC tissues and cells were evaluated through qRT-PCR and western blot, respectively. Compared with control group, FBP2 mRNA and protein levels were obviously reduced in GC tissues and cells (Fig. 7A-E). FBP2 was predicted to contain binding sites of miR-1290 by bioinformatic software starBase v2.0 (Fig. 7F). As shown in Fig. 7G,H, we designed FBP2 3′UTR-WT and FBP2 3′UTR-MUT luciferase reporter system to detect the role of miR-1290 on FBP2 expression. We found that co-transfection of miR-1290 mimics and FBP2 3′UTR-WT decreased relative luciferase activity, but not in FBP2 3′UTR-MUT system. Furthermore, FBP2 expression had an inverse correlation with miR-1290 expression and a positive correlation with circ_0026344 expression in GC (Fig. 7I,J). We further found that miR-1290 mimics down-regulated the protein level of FBP2 in AGS and HGC-27 cells, when compared with miR-NC controls (Fig. 7K,L). Circ_0026344 overexpression significantly upregulated FBP2 levels in GC cells, whereas miR-1290 mimics were able to attenuate the elevated expression of FBP2 (Fig. 7M,N). All together,

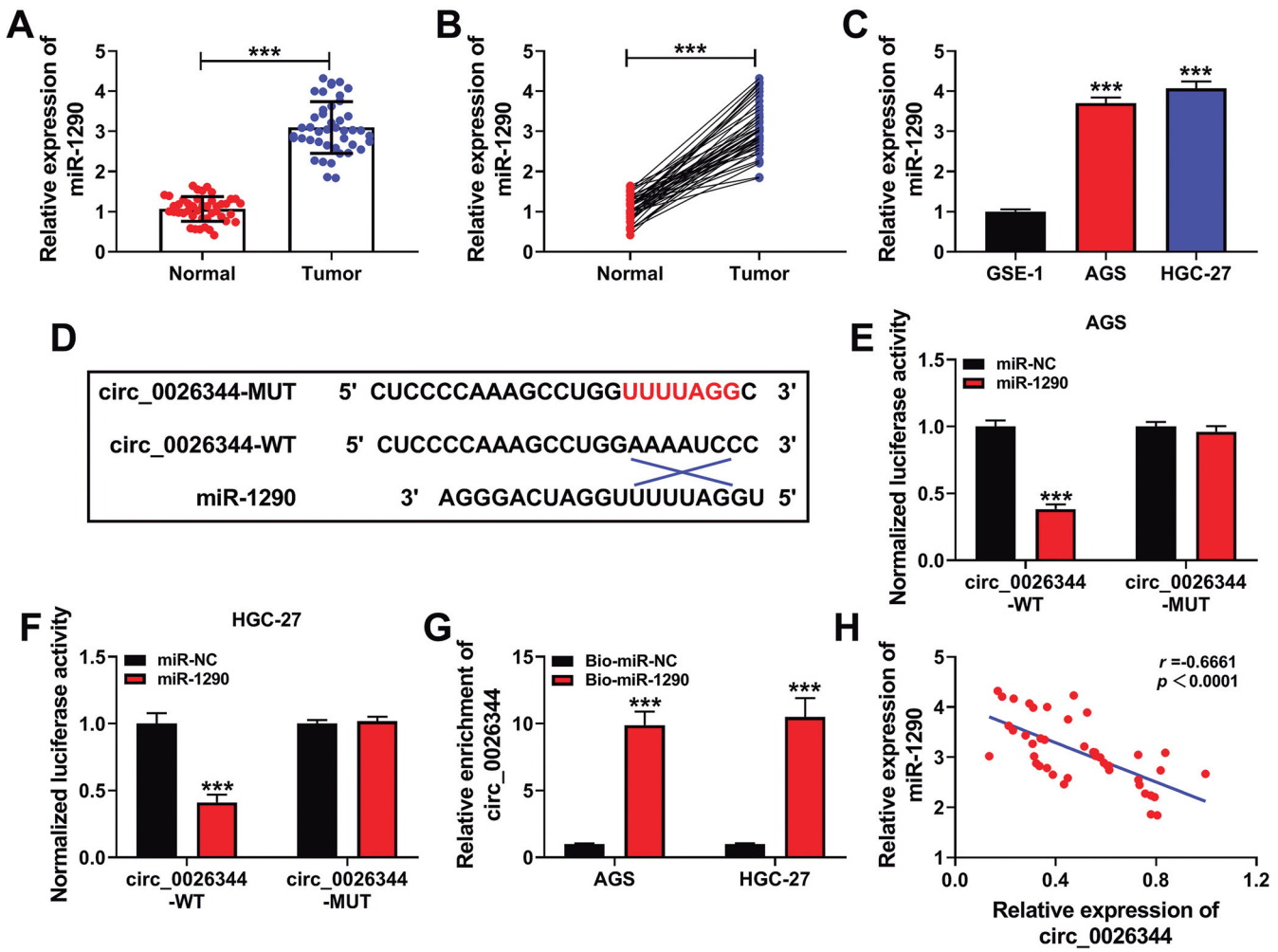

Fig. 4. Circ_0026344 and miR-1290 have a targeting relationship. **A-C.** The expression of miR-1290 in GC tissues and cells was examined using qRT-PCR. **D.** The binding site between circ_0026344 and miR-1290. **E, F.** The relationship between circ_0026344 and miR-1290 was detected by dual-luciferase reporter assay. **G.** RNA pull-down assay was used to determine the relationship between miR-1290 and circ_0026344. **H.** Pearson's correlation analysis was used to analyze the correlation between the levels of miR-1290 and circ_0026344 in GC tissues. ***P<0.001.

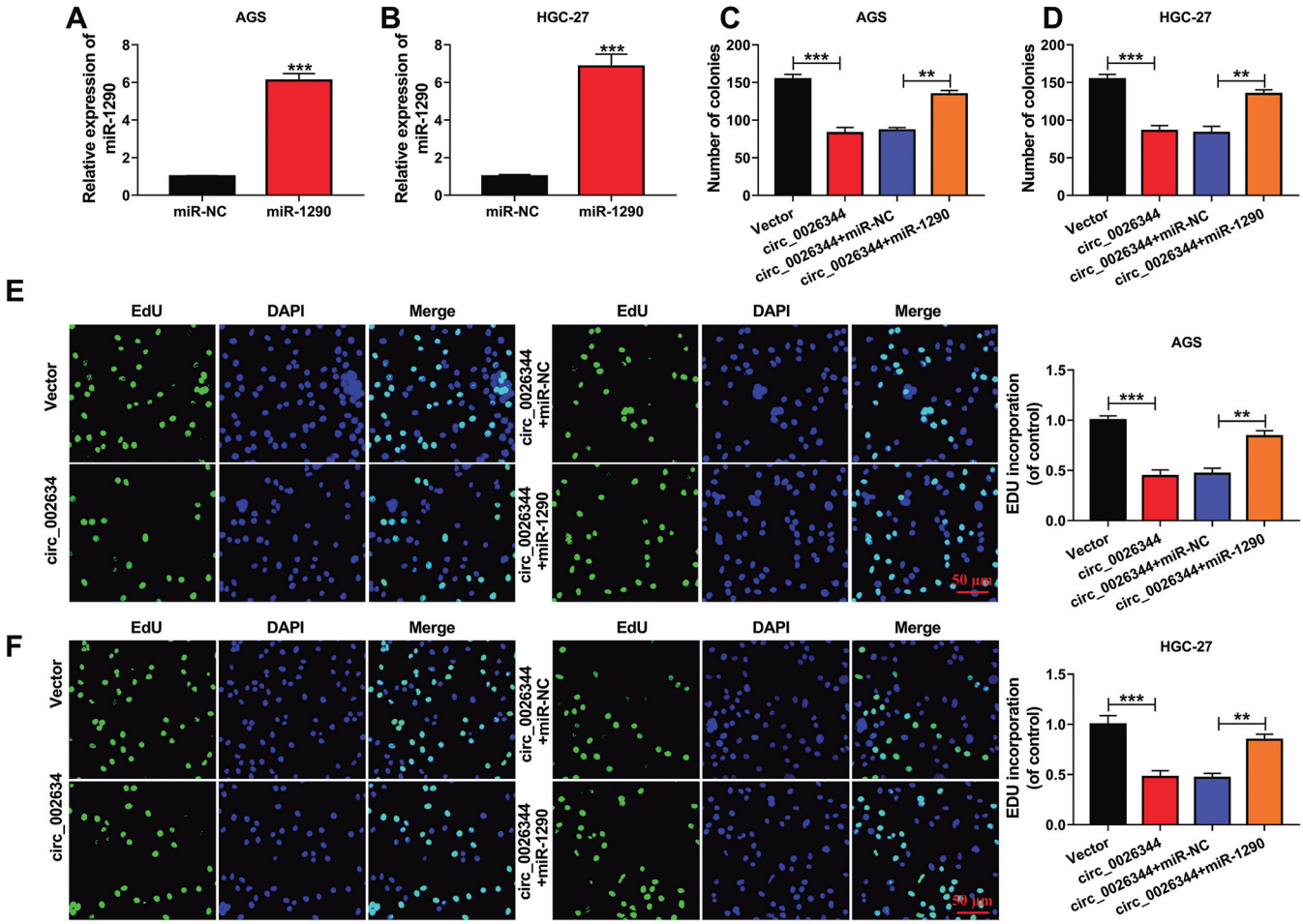

Fig. 5. miR-1290 attenuated the circ_0026344-induced anti-proliferative effects on GC cells. **A, B.** After transfection with miR-1290 mimics, the expression of miR-1290 was tested by qRT-PCR. **C, D.** Cell colony ability was assessed using colony formation assay. **E, F.** Cell proliferation was determined by EdU assay. ***P*<0.01, ****P*<0.001.

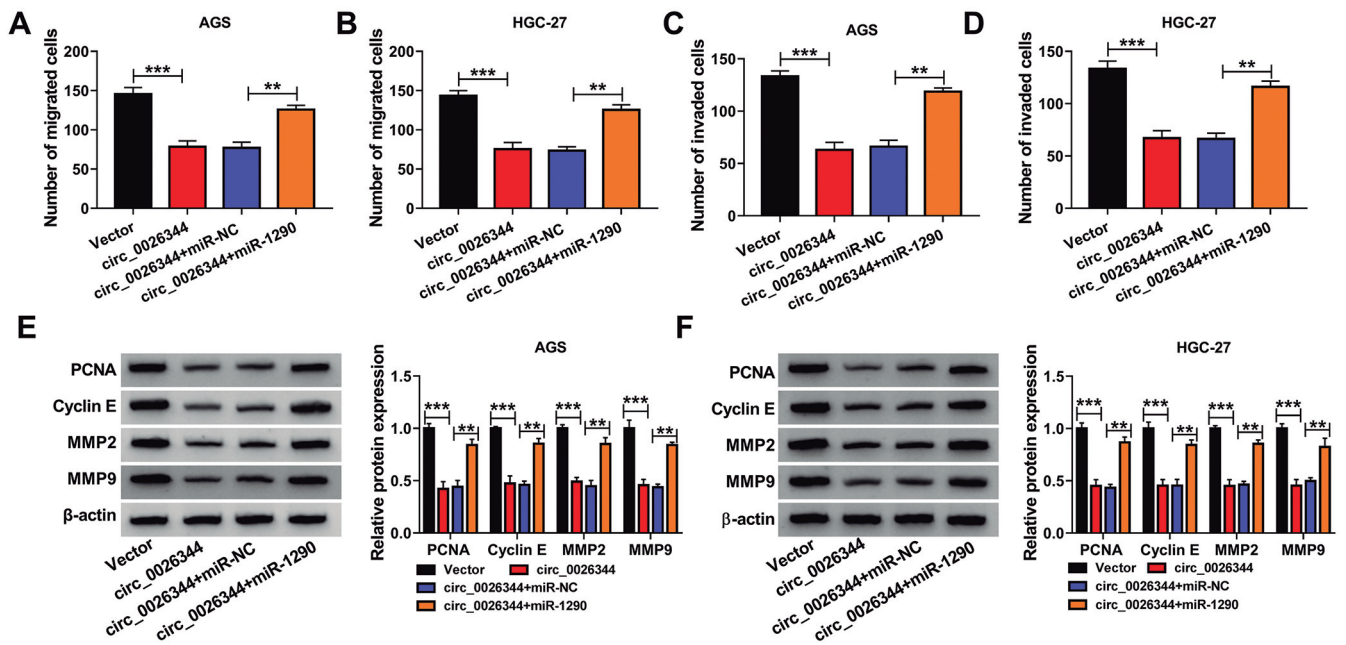

Fig. 6. miR-1290 impaired circ_0026344-induced repression of GC cell migration and invasion. **A-D.** Cell migration and invasion were determined by transwell assay. **E, F.** The Protein levels of PCNA, Cyclin E, MMP2 and MMP9 were detected by western blot. ***P*<0.01, ****P*<0.001.

these results provided evidence supporting that circ_0026344 inhibited GC cells function by regulating FBP2 expression via miR-1290.

FBP2 knockdown reversed circ_0026344 overexpression-induced anti-proliferative effect on GC cells

Rescue experiments were performed to further determine the regulatory mechanism of circ_0026344. Western blot analysis showed that si-FBP2 largely blocked the expression of FBP2 in AGS and HGC-27 cells (Fig. 8A,B). Then, AGS and HGC-27 cells were transfected with circ_0026344 or circ_0026344+si-FBP2, with Vector or circ_0026344+si-NC as the control. The number of colonies restrained by hsa_circ_0026344 overexpression was significantly recovered in circ_0026344+si-FBP2-transfected cells (Fig. 8C,D). As demonstrated in Figure 8E,F, GC cell proliferation capacity was inhibited by upregulated circ_0026344 but restored after silencing FBP2. Together, circ_0026344 played a crucial role in GC via mediating FBP2 expression.

FBP2 silencing weakened circ_0026344 upregulation-mediated effects on GC cell migration and invasion

Cell migration and cell invasion, blocked in AGS and HGC-27 cells transfected with circ_0026344, were

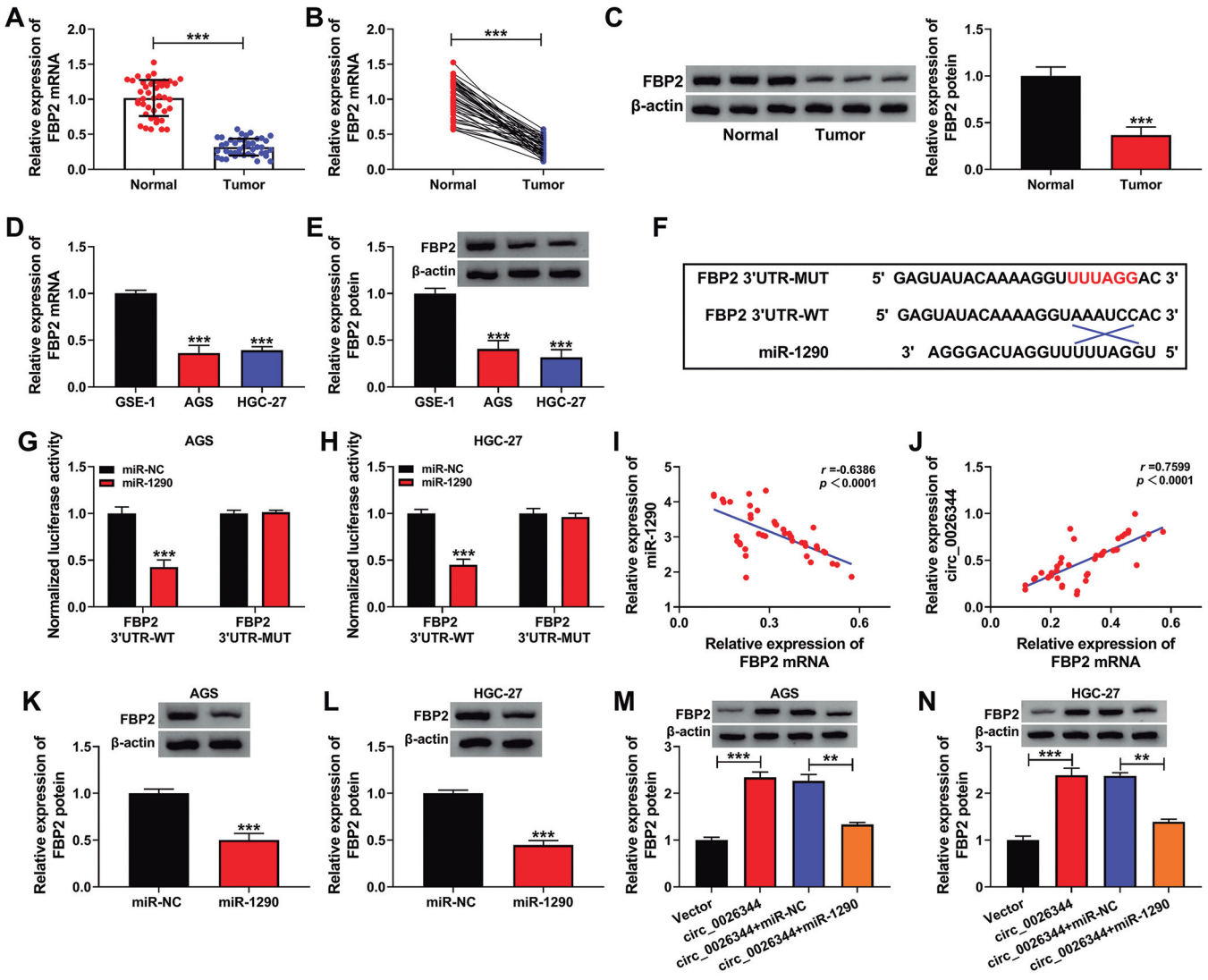

Fig. 7. FBP2 was upregulated by circ_0026344 via miR-1290. **A-E.** The mRNA and protein expressions of FBP1 in GC tissues, cells and corresponding normal tissues and cells was determined by qRT-PCR and western blot assays. **F.** The binding site between FBP2 3′UTR and miR-1290. **G, H.** The association between miR-1290 and FBP2 was verified by dual-luciferase reporter assay. **I.** Correlation analysis of miR-1290 and FBP2 in GC tissues. **J.** Correlation analysis of circ_0026344 and FBP2 in GC tissues. **K, L.** Western blot analysis was used to measure the protein level of FBP2 in AGS and HGC-27 cells. **M, N.** Western blot was used to determine FBP2 protein expression level. ***P*<0.01, ****P*<0.001.

largely facilitated in cells transfected with circ_0026344+ si-FBP2 (Fig. 9A-D). Moreover, the expression of PCNA, Cyclin E, MMP2 and MMP9 in these transfected cells was detected, and PCNA, Cyclin E, MMP2 and MMP9 expression were lessened in circ_0026344-transfected AGS and HGC-27 cells but largely recovered in circ_0026344+si-FBP2-transfected cells (Fig. 9E,F). These findings suggested that FBP2 downregulation reversed the effects of circ_0026344 overexpression, meaning that elevated circ_0026344 expression blocked GC cells development via boosting FBP2.

Circ_0026344 upregulation repressed GC growth in vivo

We further verified the role of circ_0026344 in GC *in vivo* through a xenograft assay. The results exhibited that circ_0026344 overexpression repressed tumor growth (reduced tumor volume and weight) compared to the Vector group (Fig. 10A,B). ICH results proved that compared with Vector group, Ki-67 level was abnormally impeded in circ_0026344 group (Fig. 10C). Furthermore, circ_0026344 expression was overtly elevated and miR-1290 expression was markedly reduced in tumor tissues of the circ_0026344 group when compared to the Vector group (Fig. 10D). Also, FBP2 protein was prominently upregulated in tumor tissues of the circ_0026344 group compared to that in the Vector group (Fig. 10E). These data indicated that circ_0026344 repressed BC growth *in vivo* through upregulating FBP1 via miR-1290.

Discussion

It is worth noting that the action of non-coding RNAs, covering circRNAs and microRNAs, in biological and pathological processes have attracted great attention from researchers (Isoda et al., 2019). More and more studies have uncovered that circRNAs are involved in accelerating or inhibiting tumor

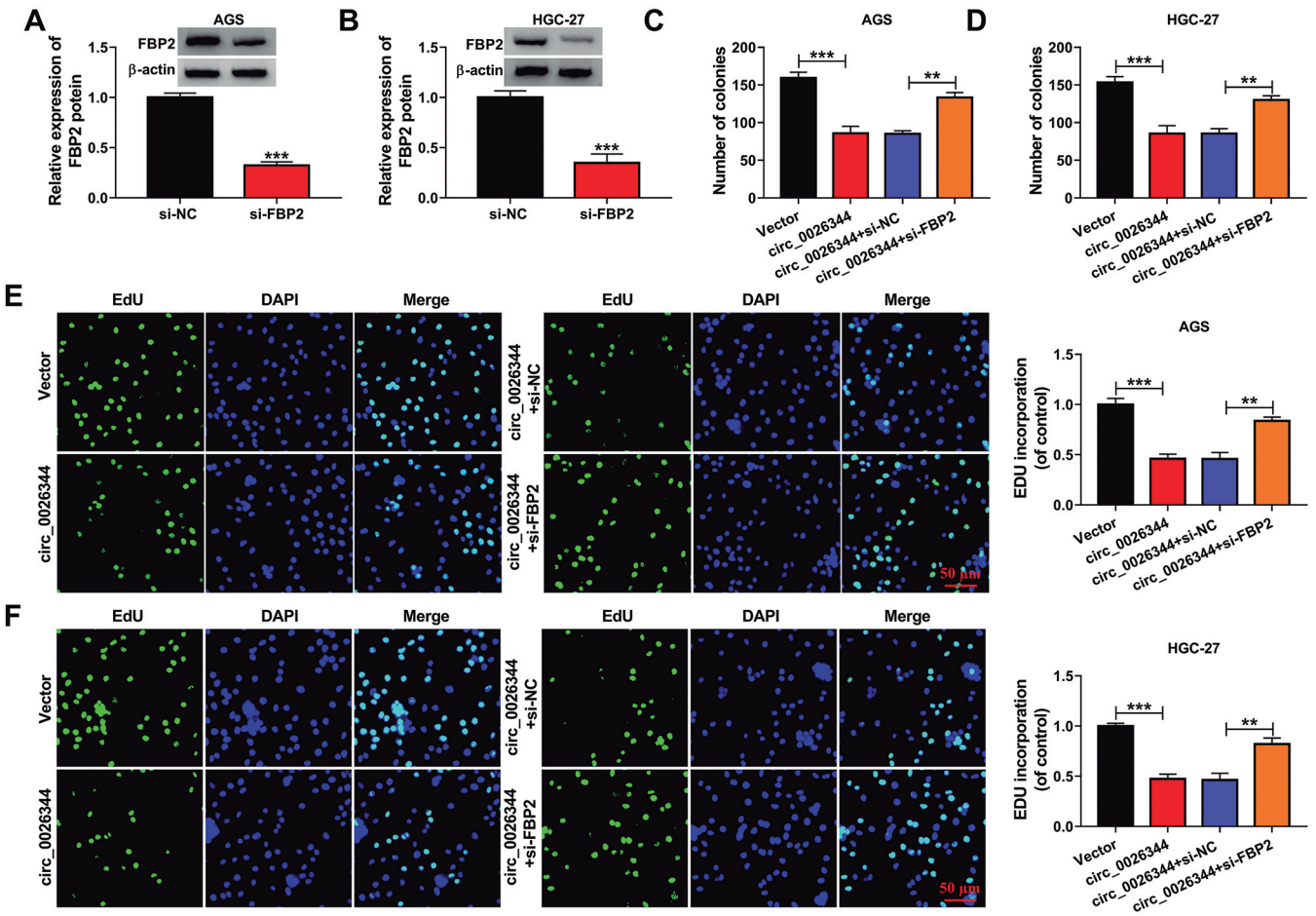

Fig. 8. Silencing of FBP2 rescued the effects of circ_0026344 overexpression on GC cell proliferation. **A, B.** The effectiveness of FBP2 knockdown was ensured by western blot. **C, D.** The ability of colony formation was examined using colony formation assay. **E, F.** Cell proliferation was monitored by EdU assay. ***P*<0.01, ***P*<0.001.

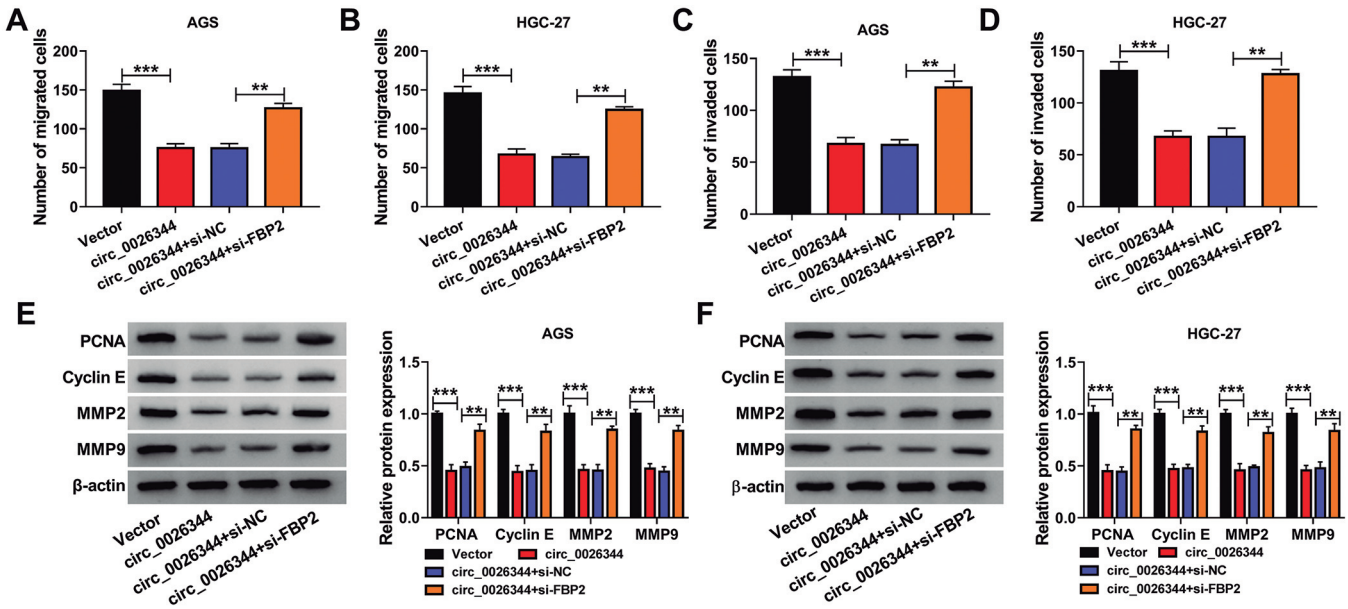

Fig. 9. FBP2 knockdown rescued the effects of circ_0026344 upregulation on GC cell migration and invasion. **A-D.** Cell migration and cell invasion were explored by transwell assay. **E-F.** The levels of PCNA, Cyclin E, MMP2 and MMP4 expression were detected by western blot. ***P*<0.01, ***P*<0.001.

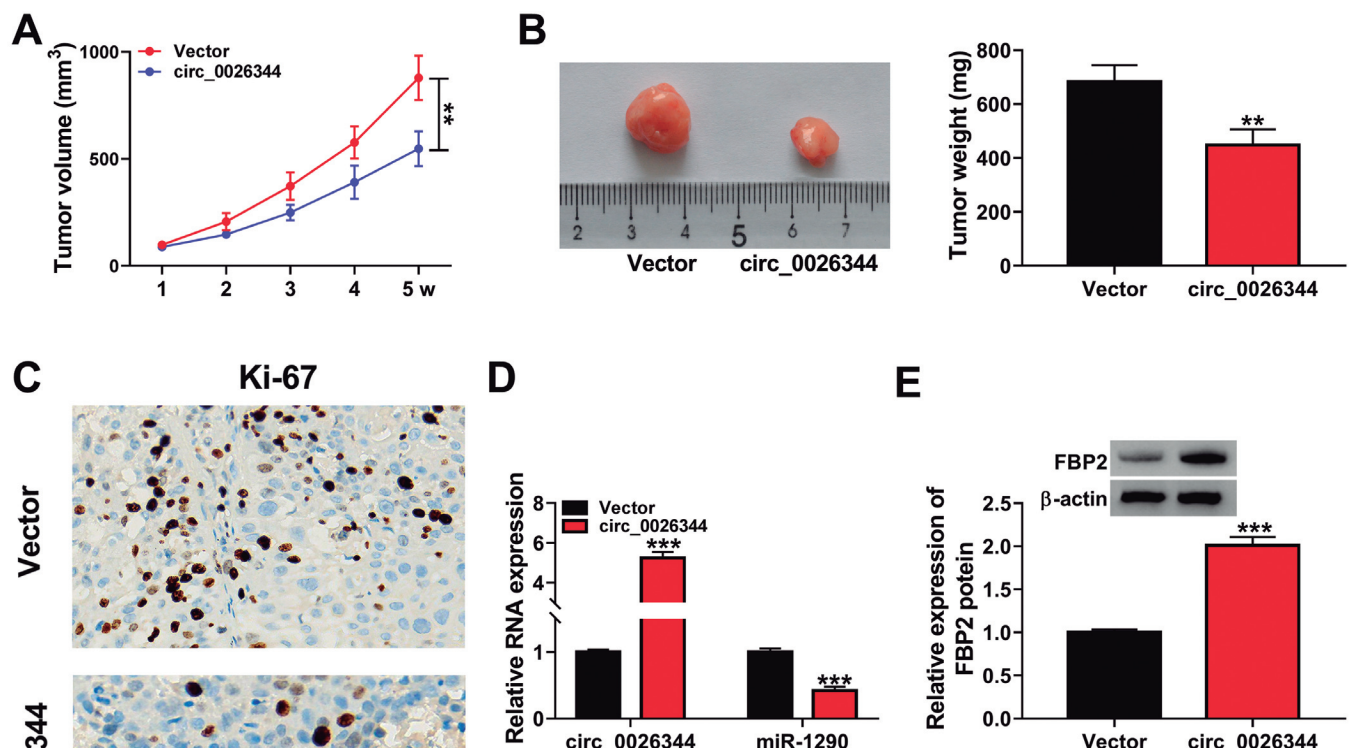

Fig. 10. Circ_0026344 overexpression repressed GC growth *in vivo*. **A.** Tumor growth curves were measured after injection of AGS cells transfected with Vector or circ_0026344. **B.** Xenograft tumors were photographed after 5 weeks of inoculation. **C.** IHC analysis was used to determine the expression of Ki67 in tumor tissues from different groups. **D.** The expression of circ_0026344 in tumor tissues of the circ_0025344 and Vector groups was analyzed by qRT-PCR. **E.** The level of FBP2 protein in tumor tissues of the circ_0026344 and Vector groups was examined with western blot analysis. ***P*<0.01, ****P*<0.001.

formation and evolution, including GC (Patop and Kadener, 2018; Li et al., 2020). For example, circDONSON has been identified as a carcinogen that promoted the occurrence and metastasis of GC (Ding et al., 2019b). Hsa_circ_0000291 has been reported to inhibit the proliferation and migration of GC cells (Cao et al., 2019). Moreover, Shen et al. claimed that circ_0026344 repressed the metastasis of colorectal cancer (Shen et al., 2019). Zhang et al. reported that circ_0026344 was downregulated in GC and was related to the tumor size, lymph node metastasis and TNM stages (Zhang et al., 2020). However, the exact roles of circ_0026344 in GC are little known. In this study, circ_0026344 was down-regulated in GC cells and tissues. In addition, the introduction of circ_0026344 inhibited cell proliferation, migration and invasion of GC cells *in vitro* and blocked tumor growth *in vivo*.

More and more data have reported that circRNAs can act as miRNA sponges to regulate miRNA expression in the cytoplasm (Chan and Tay, 2018; Zhong et al., 2018). In this study, we found that miR-1290 was the target of circ_0026344 in GC cells. In one study, miR-1290 promoted metastasis of oral squamous cell carcinoma by targeting CCNG2 (Qin et al., 2019). Previous studies have shown that miR-1290 facilitated glioma cell proliferation, migration and invasion by targeting LHX6 (Yan et al., 2018). Also, miR-1290 boosted proliferation of colorectal cancer cells via targeting INPP4B (Ma et al., 2018). Therefore, the enhanced expression of miR-1290 repressed the influence of circ_0026344 introduction on migration, invasion and proliferation of GC cells. In addition, Jin et al. believed that the up-regulation of miR-1290 promoted NSCLC cell proliferation and invasion through targeting interferon regulatory factor 2 (Jin et al., 2018). And exosome miR-1290 promoted hepatocellular carcinoma angiogenesis by targeting SMEK1 (Wang et al., 2021). Therefore, we concluded that circ_0026344 inhibited GC progression by down-regulating miR-1290.

Moreover, we confirmed that FBP2 was a target for miR-1290. FBP2 was verified to inhibit sarcoma progression via inhibiting mitochondrial biogenesis (Huangyang et al., 2020). In addition, FBP2 inhibited the progression of cervical cancer by promoting pyruvate kinase isoenzyme M2 ubiquitination and inhibiting aerobic glycolysis (Wang et al., 2022). Previous research has reported that reduced FBP2 expression can promote glycolysis and growth of GC cells (Li et al., 2013). In this work, FBP2 level was significantly decreased in GC tissues and cells. Besides, miR-1290 overexpression reversed circ_0026344-induced FBP2 upregulation in GC cells. Therefore, we concluded that circ_0026344 inhibited GC cell progression through the miR-1290/FBP2 axis.

In summary, the up-regulation of circ_0026344 blocked GC progression via adjusting the miR-1290/FBP2 axis, suggesting that circ_0026344 may be an underlying target for GC treatment. This study provides a new strategy for the treatment of patients with GC.

Acknowledgements. None.

Ethics approval and consent to participate. The present study was approved by the ethical review committee of Taihe Hospital, Hubei University of Medicine. Written informed consent was obtained from all enrolled patients. Consent for publication

Patients agree to participate in this work Availability of data and materials

The analyzed data sets generated during the present study are available from the corresponding author on reasonable request.

Authors' contribution. Conceptualization and Methodology: TingTing Zhang and BinBin Tan; Formal analysis and Data curation: BinBin Tan and Hu Hao; Validation and Investigation: GaoChun Xiao and TingTing Zhang; Writing - original draft preparation and Writing - review and editing: GaoChun Xiao, TingTing Zhang and BinBin Tan; Approval of final manuscript: all authors

Funding. No funding was received.

Disclosure of interest. The authors declare that they have no financial or non-financial conflicts of interest.

References

Allemani C., Matsuda T., Di Carlo V., Harewood R., Matz M., Nikšić M., Bonaventure A., Valkov M., Johnson C.J., Estève J., Ogunbiyi O.J., Silva G.A.E., Chen W.Q., Eser S., Engholm G., Stiller C.A., Monnereau A., Woods R.R., Visser O., Lim G.H., Aitken J., Weir H.W., Coleman M.P. and CONCORD Working Group (2018). Global surveillance of trends in cancer survival 2000-14 (CONCORD-3): analysis of individual records for 37 513 025 patients diagnosed with one of 18 cancers from 322 population-based registries in 71 countries. Lancet 391, 1023-1075.

Bray F., Ferlay J., Soerjomataram I., Siegel R.L., Torre L.A. and Jemal A. (2018). Global cancer statistics 2018: GLOBOCAN estimates of incidence and mortality worldwide for 36 cancers in 185 countries. CA Cancer J. Clin. 68, 394-424.

Cao C., Han S., Yuan Y., Wu Y., Lian W., Zhang X., Pan L. and Li M. (2019). Downregulated circular RNA hsa_circ_0000291 suppresses migration and proliferation of gastric cancer via targeting the miR-183/ITGB1 axis. Cancer Manag. Res. 11, 9675-9683.

Chan J.J. and Tay Y. (2018). Noncoding RNA:RNA regulatory networks in cancer. Int. J. Mol. Sci. 19, 1310.

Ding H., Shi Y., Liu X. and Qiu A. (2019a). MicroRNA-4513 promotes gastric cancer cell proliferation and epithelial-mesenchymal transition through targeting KAT6B. Hum. Gene Ther Clin. Dev. 30, 142-148.

Ding L., Zhao Y., Dang S., Wang Y., Li X., Yu X., Li Z., Wei J., Liu M. and Li G. (2019b). Circular RNA circ-DONSON facilitates gastric cancer growth and invasion via NURF complex dependent activation of transcription factor SOX4. Mol. Cancer 18, 45.

Funakoshi T., Miyamoto S., Kakiuchi N., Nikaido M., Setoyama T., Yokoyama A., Horimatsu T., Yamada A., Torishima M., Kosugi S., Yamada H., Sugimura H., Haga H., Sakai Y., Ogawa S., Seno H., Muto M. and Chiba T. (2019). Genetic analysis of a case of *Helicobacter pylori*-uninfected intramucosal gastric cancer in a family with hereditary diffuse gastric cancer. Gastric Cancer 22, 892-898.

Ge S., Feng X., Shen L., Wei Z., Zhu Q. and Sun J. (2012). Association between habitual dietary salt intake and risk of gastric cancer: A systematic review of observational studies. Gastroenterol. Res. Pract. 2012, 808120.

Ge L., Wang Y., Duan Q.H., Liu S.S. and Liu G.J. (2019). MicroRNA-760 acts as a tumor suppressor in gastric cancer development via inhibiting G-protein-coupled receptor kinase interacting protein-1 transcription. World J. Gastroenterol. 25, 6619-6633.

Gong Y., Mao J., Wu D., Wang X., Li L., Zhu L. and Song R. (2018). Circ-ZEB1.33 promotes the proliferation of human HCC by sponging miR-200a-3p and upregulating CDK6. Cancer Cell Int. 18, 116.

Hu M.L., Xiong S.W., Zhu S.X., Xue X.X. and Zhou X.D. (2019). MicroRNAs in gastric cancer: from bench to bedside. Neoplasma 66, 176-186.

Huangyang P., Li F., Lee P., Nissim I., Weljie A.M., Mancuso A., Li B., Keith B., Yoon S.S. and Simon M.C. (2020). Fructose-1,6-Bisphosphatase 2 Inhibits sarcoma progression by restraining mitochondrial biogenesis. Cell Metabol. 31, 1032.

Isoda T., Morio T. and Takagi M. (2019). Noncoding RNA transcription at enhancers and genome folding in cancer. Cancer Sci. 110, 2328-2336.

Jin J.J., Liu Y.H., Si J.M., Ni R. and Wang J. (2018). Overexpression of miR-1290 contributes to cell proliferation and invasion of non small cell lung cancer by targeting interferon regulatory factor 2. Int. J. Biochem. Cell Biol. 95, 113-120.

Li H., Wang J., Xu H., Xing R., Pan Y., Li W., Cui J., Zhang H. and Lu Y. (2013). Decreased fructose-1,6-bisphosphatase-2 expression promotes glycolysis and growth in gastric cancer cells. Mol. Cancer 12, 110.

Li R., Jiang J., Shi H., Qian H., Zhang X. and Xu W. (2020). CircRNA: a rising star in gastric cancer. Cell Mol. Life Sci. 77, 1661-1680.

Ma Q., Wang Y., Zhang H. and Wang F. (2018). miR-1290 contributes to colorectal cancer cell proliferation by targeting INPP4B. Oncol. Res. 26, 1167-1174.

Meng L., Chen Z., Jiang Z., Huang T., Hu J., Luo P., Zhang H., Huang M., Huang L., Chen Y., Lu M. and Xu A-Man. (2020). MiR-122-5p suppresses the proliferation, migration, and invasion of gastric cancer cells by targeting LYN. Acta Biochim. Biophys. Sin. (Shanghai). 52, 49-57.

Miao X., Xi Z., Zhang Y., Li Z., Huang L., Xin T., Shen R. and Wang T. (2020). Circ-SMARCA5 suppresses colorectal cancer progression via downregulating miR-39-3p and upregulating ARID4B. Dig. Liver Dis. 52, 1494-502.

Ouyang Y., Li Y., Huang Y., Li X., Zhu Y., Long Y., Wang Y., Guo X. and Gong K. (2019). CircRNA circPDSS1 promotes the gastric cancer progression by sponging miR-186-5p and modulating NEK2. J. Cell Physiol. 234, 10458-10469.

Patop I.L. and Kadener S. (2018). circRNAs in cancer. Curr. Opin. Genet. Dev. 48, 121-127.

Qin W.J., Wang W.P., Wang X.B., Zhang X.T. and Du J.D. (2019). MiR-1290 targets CCNG2 to promote the metastasis of oral squamous cell carcinoma. Eur. Rev. Med. Pharmacol. Sci. 23, 10332-10342.

Qu S., Yang X., Li X., Wang J., Gao Y., Shang R., Sun W., Dou K. and Li H. (2015). Circular RNA: A new star of noncoding RNAs. Cancer Lett. 365, 141-148.

Qu S., Zhong Y., Shang R., Zhang X., Song W., Kjems J. and Li H. (2017). The emerging landscape of circular RNA in life processes. RNA Biol. 14, 992-999.

Shen T., Cheng X., Liu X., Xia C., Zhang H., Pan D., Zhang X and Li Y. (2019). Circ_0026344 restrains metastasis of human colorectal cancer cells via miR-183. Artif. Cells Nanomed. Biotechnol. 47, 4038-4045.

Shen Y., Zhang M., Da L., Huang W. and Zhang C. (2020). Circular RNA circ_SETD2 represses breast cancer progression via modulating the miR-155-5p/SCUBE2 axis. Open Med. (Wars). 15, 940-953.

Sun D., Wang G., Xiao C. and Xin Y. (2021). Hsa_circ_001988 attenuates GC progression in vitro and in vivo via sponging miR-197-3p. J. Cell Physiol. 236, 612-24.

Vainio H., Heseltine E. and Wilbourn J. (1994). Priorities for future IARC monographs on the evaluation of carcinogenic risks to humans. Environ. Health Perspect. 102, 590-591.

Wang Q., Wang G., Niu L., Zhao S, Li J., Zhang Z., Jiang H., Zhang Q., Wang H., Sun P., Xiang R, Chang A. and Yang S. (2021). Exosomal miR-1290 promotes angiogenesis of hepatocellular carcinoma via targeting SMEK1. J. Oncol. 2021, 6617700.

Wang B., Yuan Y., Zou Y., Qi Z., Huang G., Liu Y., Xia S., Huang Y. and Huang Z. (2022). Fructose-1,6-bisphosphatase 2 represses cervical cancer progression via inhibiting aerobic glycolysis through promoting pyruvate kinase isozyme type M2 ubiquitination. Anticancer Drugs. 33, e198-e206.

Wei Y., Wang Y., Zang A., Wang Z., Fang G. and Hong D. (2019). MiR-4766-5p inhibits the development and progression of gastric cancer by targeting NKAP. Onco. Targets Ther. 12, 8525-8536.

Yan L., Cai K., Sun K., Gui J. and Liang J. (2018). MiR-1290 promotes proliferation, migration, and invasion of glioma cells by targeting LHX6. J. Cell Physiol. 233, 6621-6629.

Zhang J., Liu H., Hou L., Wang G., Zhang R., Huang Y., Chen X. and Zhu J. (2017). Circular RNA_LARP4 inhibits cell proliferation and invasion of gastric cancer by sponging miR-424-5p and regulating LATS1 expression. Mol. Cancer 16, 151.

Zhang X., Zhang L., Cui L., Chen M., Liu D. and Tian J. (2020). Expression of circRNA circ_0026344 in gastric cancer and its clinical significance. Int. J. Clin. Exp. Pathol. 13, 1017-1023.

Zhong Y., Du Y., Yang X., Mo Y., Fan C., Xiong F., Ren D., Ye X., Li C., Wang Y., Wei F., Guo C., Wu X., Li X., Li Y., Li G., Zeng Z. and Xiong W. (2018). Circular RNAs function as ceRNAs to regulate and control human cancer progression. Mol. Cancer 17, 79.

Accepted November 28, 2022